Kolmogorov-Arnold Networks Based Signal Detection for OTFS Systems in LEO Satellite Communications

Yakai Zhang[1], Jiayi He[1], and Zhiyong Liu[1,2,3(✉)]

[1] School of Information Science and Engineering of HIT, Weihai 264209, China
lzyhit@hit.edu.cn
[2] Shandong Provincial Key Laboratory of Marine Electronic Information and Intelligent Unmanned Systems, Weihai 264209, China
[3] Key Laboratory of Cross-Domain Synergy and Comprehensive Support for Unmanned Marine Systems of Ministry of Industry and Information Technology, Weihai 264209, China

Abstract. In numerous studies, orthogonal time-frequency space (OTFS) has been utilized in satellite-terrestrial communication systems with high mobility due to its strong adaptability to Doppler shifts and delays. Signal detection, a crucial technology influencing OTFS performance, is often hindered by high complexity or suboptimal detection capabilities. To address this, we propose a Kolmogorov-Arnold Networks (KANs)-based OTFS signal detection method for low Earth orbit satellite (LEO-Sat) communication systems. KANs employ learnable activation functions instead of traditional learnable linear weights between network nodes, enabling dynamic activation functions to enhance model accuracy. We integrate KANs, trained offline, into the LEO-Sat system to recover distorted signals at the receiver, facilitating effective signal detection. Compared to conventional detection algorithms, the proposed method demonstrates superior Bit Error Rate (BER) performance. Additionally, KANs are more parameter-efficient than DNNs, using significantly fewer parameters.

Keywords: OTFS · Kolmogorov-Arnold networks(KANs) · satellite · signal detection

1 Introduction

Unlike traditional terrestrial communication systems, low Earth orbit satellite (LEO-Sat) communications provide extensive coverage unimpeded by terrain,

This research was partially funded by the National Natural Science Foundation of China under Grant 61871148; the Major Scientific and Technological Innovation Project of Shandong Province under Grants 2020CXGC010705, 2021ZLGX05, and 2022ZLGX04; and the Strategic Rocketry Innovation Fund Project under Grant ZH2022007.

H.-H. Chen and W. Meng (Eds.): WiSATS 2024, LNICST 605, pp. 138–149, 2025.
https://doi.org/10.1007/978-3-031-86196-3_12

ensuring reliable services in remote and underdeveloped regions. This capability makes it an essential element of the next-generation global communication network [1]. However, the LEO satellite-terrestrial communication environment differs significantly from terrestrial systems due to high Doppler shift characteristics that disrupt subcarrier orthogonality in conventional OFDM systems, resulting in considerable performance degradation [2]. Recently, the orthogonal time-frequency space (OTFS) 2D modulation technique has been introduced, converting time-varying channels into nearly time-invariant ones in the delay-Doppler (DD) domain. This conversion enables data symbols to be multiplexed in this stable DD domain [3, 4], effectively combating Doppler frequency shift interference and greatly enhancing system performance. Studies in references [5–8] have shown that OTFS performs better than OFDM in satellite-terrestrial high dynamics scenarios.

Signal detection is a crucial technology influencing the performance of LEO-Sat communication systems utilizing OTFS. Traditional detection methods are typically divided into linear and nonlinear algorithms. Linear methods include the Minimum Mean Square Error (MMSE) algorithm [9] and the Zero Forcing (ZF) algorithm [10], both requiring matrix inversion and having high computational complexity. Nonlinear approaches involve the Markov Monte Carlo detection algorithm [11] and the message passing detection algorithm [12]. However, the former does not exploit the sparse nature of the channel in the delay-Doppler (DD) domain and also has high complexity. In contrast, the latter approximates the interference term as Gaussian noise, which does not accurately reflect the actual interference distribution in satellite-ground communication systems, leading to performance degradation.

In wireless communication systems, algorithms based on deep learning exhibit strong nonlinear representation capabilities, enabling effective detection in non-ideal assumption models [13]. Research [14–16] has utilized different neural networks, including DNN, CNN, and LSTM, for OTFS signal detection, resulting in better bit error rate (BER) performance than conventional approaches. Specifically, reference [14] proposed two DNN-based detection strategies: one utilizes a fully connected DNN to frame the detection task as a multi-class classification problem, while the other employs multiple DNNs, each responsible for detecting an individual symbol within the transmission vector. Reference [15] implemented the MP algorithm to preprocess the two-dimensional OTFS frame signal at the receiver, subsequently feeding it into a two-dimensional CNN for detection, resulting in a BER performance nearly identical to that of the MAP detector but with reduced complexity. Furthermore, reference [16] proposed a Bi-LSTM-based detection method for underwater OTFS signals, resulting in a lower symbol error rate (SER) compared to traditional algorithms. Despite these advancements, all the aforementioned neural networks rely on Multi-Layer Perceptron (MLP) architecture with fixed activation functions at the nodes and linear functions along the edges [17], which leads to low convergence speeds and increased model complexity.

A recent study [17] introduced Kolmogorov-Arnold Networks (KANs), an innovative neural network architecture aimed at replacing conventional MLPs. Unlike MLPs, which rely on the universal approximation theorem, KANs are grounded in the Kolmogorov-Arnold representation theorem [18,19] and utilize learnable activation functions instead of conventional linear weights between nodes. In KANs, fixed activation functions are replaced by additive operations, resulting in a faster neural scaling law, enhanced accuracy, and improved interpretability. Notably, KANs can achieve similar or better prediction results than MLPs while using a smaller network size. Reference [20] shows that KANs are effective for time series prediction, offering more precise results than traditional MLPs with fewer parameters. Nevertheless, to the best of the authors' knowledge, applying KANs for signal detection in OTFS systems within LEO satellite communications remains unexplored.

Given the benefits of OTFS and the exceptional capabilities of KANs, this paper proposes an OTFS signal detection algorithm for the LEO-Sat system, utilizing KANs to enhance the overall performance of satellite-terrestrial communication systems.

2 System Model

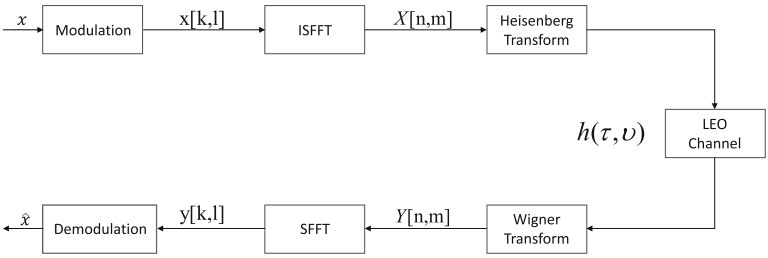

Fig. 1. OTFS based LEO-Sat communication system block diagram.

2.1 Basic Principle of OTFS

Figure 1 presents the block diagram of the LEO-Sat communication system utilizing OTFS. At the transmitter, binary bit information x is modulated into DD domain symbol $x[k,l]$, where $k = 0,1,2,...,N-2,N-1; l = 0,1,2,...,M-2,M-1$, These DD domain signals are organized into squares to create a frame of OTFS symbols. Each OTFS symbol undergoes an inverse symplectic finite Fourier transform (ISFFT) to yield the time-frequency(TF) domain symbol $X[n,m]$:

$$X[n,m] = \frac{1}{\sqrt{MN}} \sum_{k=0}^{N-1} \sum_{l=0}^{M-1} x[k,l] e^{j2\pi(\frac{nk}{N} - \frac{nl}{M})} \tag{1}$$

The time-frequency (TF) domain signals are mapped to the time domain transmitted signal $s(t)$ using the Heisenberg transform along with windowing techniques:

$$s(t) = \sum_{n=0}^{N-1} \sum_{m=0}^{M-1} X[n,m] g_{tx}(t - nT) e^{j2\pi m\Delta f(t-\Delta f)} \tag{2}$$

where g_{tx} represents the transmit pulse, T indicates the duration of the subframe, and $\Delta f = 1/T$ signifies the subcarrier interval.

The channel impulse response in the DD domain can be articulated as follows:

$$h(\tau, \upsilon) = \sum_{i=1}^{p} h_i \delta(\tau - \tau_i)\delta(\upsilon - \upsilon_i) \tag{3}$$

where h_i represents the channel gain of the i^{th} path, while τ_i and υ_i denote the time delay and frequency offset of the i^{th} path, respectively. The values of τ_i and υ_i can be determined by

$$\tau_i = \frac{l_i}{M\Delta f}, \nu_i = \frac{k_i + \kappa_i}{NT} \tag{4}$$

where k_i and κ_i represent the integer and fractional Doppler indices of the i^{th} path, respectively.

The transmitted symbols arrive at the receiver after traversing the channel characterized by the above impulse response, and the received symbols can be expressed as follows:

$$r(t) = \int_{\nu} \int_{\tau} h(\tau, \nu) s(t - \tau) e^{j2\pi\nu(t-\tau)} d\tau d\nu + n(t) \tag{5}$$

where $n(t)$ represents the additive white Gaussian noise. Plugging Eq. (3) into Eq. (4):

$$r(t) = \sum_{i=1}^{p} h_i e^{j2\pi\nu_i(t-\tau_i)} s(t - \tau_i) + n(t) \tag{6}$$

By sampling at $t = nT$ and $f = m\Delta f$, the received symbols are transformed into the TF domain symbols using the Wenger transform:

$$Y[n,m] = \int g^*_{rx}(t - nT) r(t) e^{-j2\pi m\Delta f(t-nT)} dt \tag{7}$$

where g_{rx} denotes the receive pulse. The TF domain symbols $Y[n,m]$ are converted to the DD domain signal using the symplectic finite Fourier transform (SFFT):

$$y[k,l] = \frac{1}{\sqrt{MN}} \sum_{n=0}^{N-1} \sum_{m=0}^{M-1} Y[n,m] e^{-j2\pi(\frac{nk}{N} - \frac{ml}{M})} \tag{8}$$

Ultimately, the binary data information $\hat{x}$ is derived through equalization and demodulation of the DD domain symbols at the receiver.

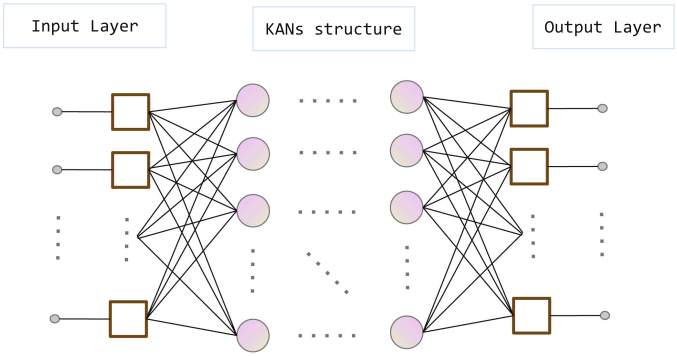

Fig. 2. Multiple-input multiple-output KAN network structure diagram.

2.2 Kolmogorov-Arnold Networks (KANs)

The Kolmogorov-Arnold representation theorem, independently developed by Andrey Kolmogorov and Vladimir Arnold, states that any multivariate continuous function u defined on a bounded domain can be represented as a finite composition of single-variable continuous functions combined with the operation of addition [18]. Specifically, for a smooth function $u : [0,1]^n \to \mathbb{R}$,

$$u(\mathbf{x}) = u(x_1, \cdots, x_n) = \sum_{p=1}^{2n+1} \Phi_p \left(\sum_{q=1}^{n} \phi_{p,q}(x_q) \right) \tag{9}$$

where $\Phi_p : \mathbb{R} \to \mathbb{R}$ and $\phi_{p,q} : [0,1] \to \mathbb{R}$. Inspired by Kolmogorov-Arnold representation theorem, literature [17] proposed Kolmogorov-Arnold network architecture. The network structure is shown in Fig. 2, the width and depth of the network are arbitrary, and the nodes represent additive operations, while the connections between them utilize learnable activation functions. In reference [17], the learnable activation function is defined as a B-spline function, where the spline curve is a smooth, continuous curve defined by a series of control nodes. This is defined by the order k and the number of intervals G. The parameter k indicates the order of the polynomial function used to approximate the curve between control nodes, while G specifies the number of subintervals between adjacent control points. The l^{th} KAN layer can be represented as the function matrix Φ_p composed by univariate functions $\phi_{p,q}(\cdot)$ with $p = 1, 2, 3, ..., N_{in}$ and $q = 1, 2, 3, ..., N_{out}$, where N_{in} and N_{out} denote the dimension of inputs and outputs, respectively, and $\phi_{p,q}(\cdot)$ are the trainable spline functions. The structure of a KAN is represented by an integer array $[n_0, n_1, n_2, n_3, ..., n_{L-1}, n_L]$. A general KAN network consists of L layers:

$$\mathrm{y} = u_{KAN}(\mathbf{x}) = (\mathbf{\Phi}_{L-1} \circ \cdots \circ \mathbf{\Phi}_0)\mathbf{x} \tag{10}$$

It is essential to highlight that above operations are differentiable, enabling KANs to be trained through backpropagation.

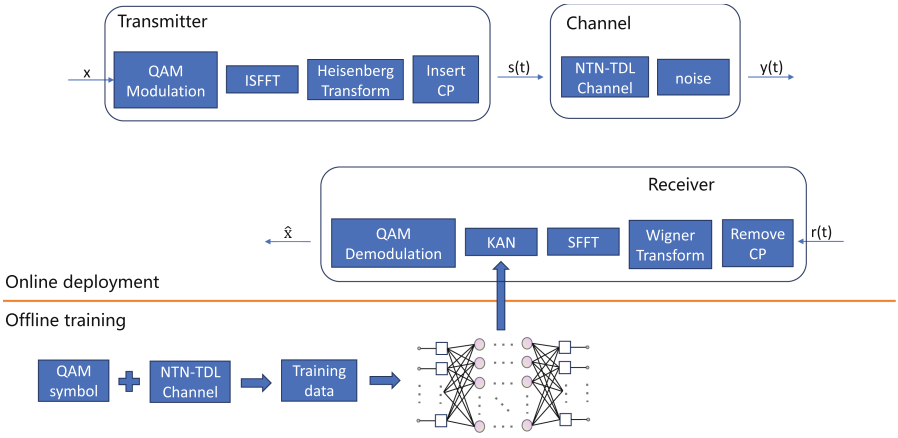

Fig. 3. KANs based OTFS signal detection in LEO-Sat system structure diagram.

3 KANs Based OTFS Signal Detection in LEO-Sat System

Figure 3 presents the system block diagram for the OTFS signal detection algorithm designed for the LEO-Sat system, which utilizes a KAN network. The transmitter operates similarly to a conventional OTFS system; however, a signal detection module based on the KAN network is integrated at the receiver to identify the distorted signal. The system model is organized into two stages. In the first stage, the OTFS samples generated by the model are used to train the KAN network. The second stage involves online deployment, where the trained KAN network is employed to recover the original transmitted data in the OTFS system, enabling effective signal detection.

During the model training phase, the transmitter generates pseudo-random input data and subsequently travels through the channel to reach the receiver, resulting in the received signal. The original transmitted data and the received signal y together constitute the training data set. The model is trained to minimize the discrepancies between the neural network's output and the transmitted data, represented by a loss function $L(loss)$:

$$L(loss) = \frac{1}{M} \sum_{j=0}^{M-1} (\hat{x}(j) - x(j))^2 \tag{11}$$

The system model is composed of MN data symbols within a frame, where both the real and imaginary parts of each symbol serve as input to the network. The output of the network consists of $2MN$ data, corresponding to the real and imaginary components of the MN symbols. Training and testing of the network are carried out using the PyTorch framework.

4 Numberical Results

4.1 System Setup

To assess the performance of the proposed OTFS signal detection algorithm for the LEO-Sat communication system utilizing KANs, this section computes the bit error rate (BER) through MATLAB simulations and contrasts it with traditional methods such as ZF, MMSE, and DNN. The channel model employs the NTN-TDL-D model as outlined in the 3GPP TR 38.811 protocol [21], with channel parameters presented in Table 1. This model features three taps: the first tap follows a Rician distribution with a K factor of 11.707 dB, while the remaining two taps adhere to a NLOS Rayleigh fading distribution.

Table 1. The power delay profile of the LEO-Sat communication channel.

Tap	delay	Power(dB)	Fading distribution
1	0	−0.284	Rician
	0	−11.991	Rayleigh
2	0.5596	−9.887	Rayleigh
3	7.3340	−16.771	Rayleigh

The parameters of the LEO-Sat system are presented in Table 2. In the LEO-Sat channel model, the Doppler shift for each tap is determined using the formula [22]:

$$f_d = (f_{\text{sat}} + f_c)\frac{V_t}{c}\cos\alpha\cos\phi, \quad f_{\text{sat}} = \frac{f_c\nu_{\text{sat}}}{c}\cdot\frac{R}{R+h}\cos\alpha \tag{12}$$

where c represents the speed of light, h is the altitude of the LEO satellite, α indicates the elevation angle of the LEO satellite, f_c is the carrier frequency, R denotes the Earth's radius, and ϕ is the angle between the direction of the user's equipment (UE) movement and the satellite's projected plane. Utilizing the parameters mentioned above, the model system generates 50,000 frames of training data, with the size ratio of the training set, validation set, and test set being 4:1:1. The structure of the KANs presented in this paper is [256, 256], which can be expressed as follows:

$$\mathbf{y} = \text{KAN}(\mathbf{x}) = \mathbf{\Phi x} \tag{13}$$

The DNN architecture consists of 4 layers, with the number of neurons in each layer being 256, 512, 512, and 256, respectively, and the activation function employed is LeakyReLU. The loss function utilized is MSELoss. All networks were trained for 500 epochs with the Adam optimizer, and the learning rate is 0.001.

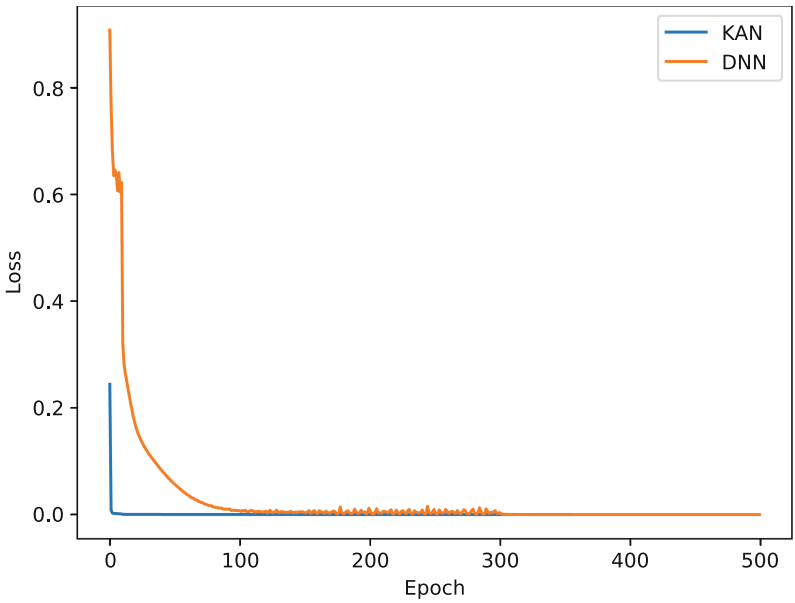

Fig. 4. Comparison of convergence speed of KAN and DNN loss functions on the validation dataset.

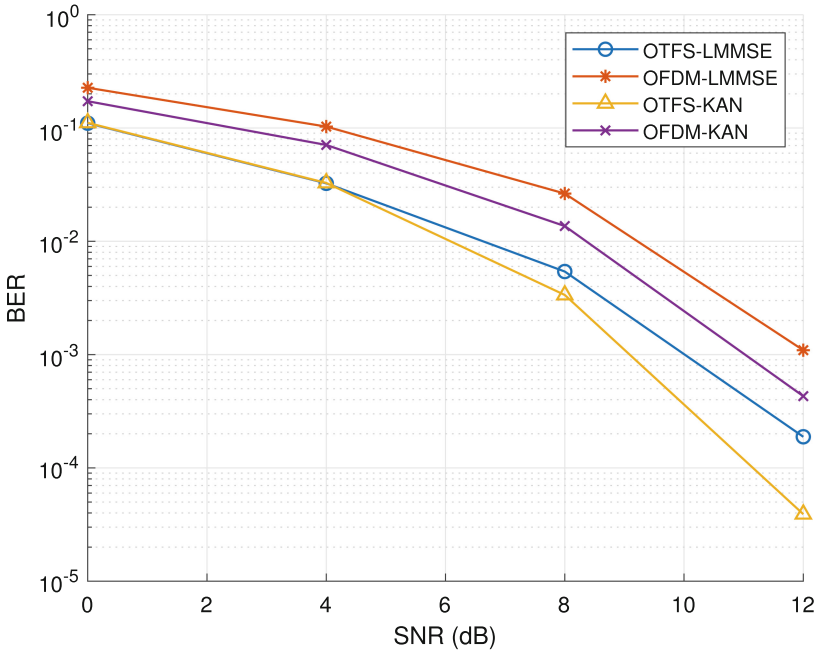

Fig. 5. 4-QAM BER performance comparison of the OTFS and OFDM in LEO-Sat system, $M = 16, N = 8, CP = 5$.

Table 2. Parameters for OTFS in LEO-Sat system.

Parameter	Value
Earth radius, R	6371 km
Satellite height, h	1500 km
Elevation angle, α	50^o
User Moving Direction, ϕ	40^o
Satellite speed, v_{sat}	7.11 km/s
UE speed, V_t	500 km/hr
Carrier frequency, f_c	20 GHz
Subcarrier frequency, Δf	60 kHz

4.2 Simulation Results

Figure 4 illustrates the trend of the loss function for both KAN and DNN as training epochs grows on the validation dataset. The blue curve indicates the loss function of the KAN, while the orange curve represents that of the DNN. The KAN network achieves convergence around 5 training epochs, whereas the DNN converges approximately at 100 epochs, demonstrating that the KAN converges more quickly than the DNN. This increased speed is attributed to the learnable activation function of the KAN, which allows for more efficient learning of the intrinsic data relationships compared to the DNN.

To validate the BER performance of the proposed algorithm, KAN, DNN, LMMSE, and ZF algorithms are employed for OTFS signal detection in LEO-Sat system.

Figure 5 illustrates the BER performance comparison of OTFS and OFDM with KAN and LMMSE. It shows that whether KAN or LMMSE, OTFS performance is better than OFDM, and KAN performance is better than LMMSE. Specifically, at BER $= 1 \times 10^{-3}$, the OTFS performance gain both are about 2 dB compared to OFDM with KAN and LMMSE. This is because that high speed satellite motion generates high Doppler shift, while OTFS transmits data in the DD domain and its resistance to Doppler interference is higher than OFDM.

Figure 6 presents the BER performance comparison of OTFS signal detection using different algorithms within the LEO-Sat communication system. The simulation results demonstrate that the proposed detection algorithm outperforms the others across all SNR levels. Specifically, both the KAN and DNN algorithms, which are based on deep learning, show improved performance compared to the traditional ZF and LMMSE algorithms as SNR increases, with the KAN algorithm achieving better BER performance than DNN. Notably, targeting the BER of 1.1×10^{-4}, the KAN achieves a gain of approximately 1 dB over DNN. This advantage arises because KAN employs nonlinear kernel functions to replace linear functions on the edges of the DNN, incorporating learnable activation functions between nodes and substituting fixed activation functions with simple addition operations. This adjustment enhances KAN's prediction

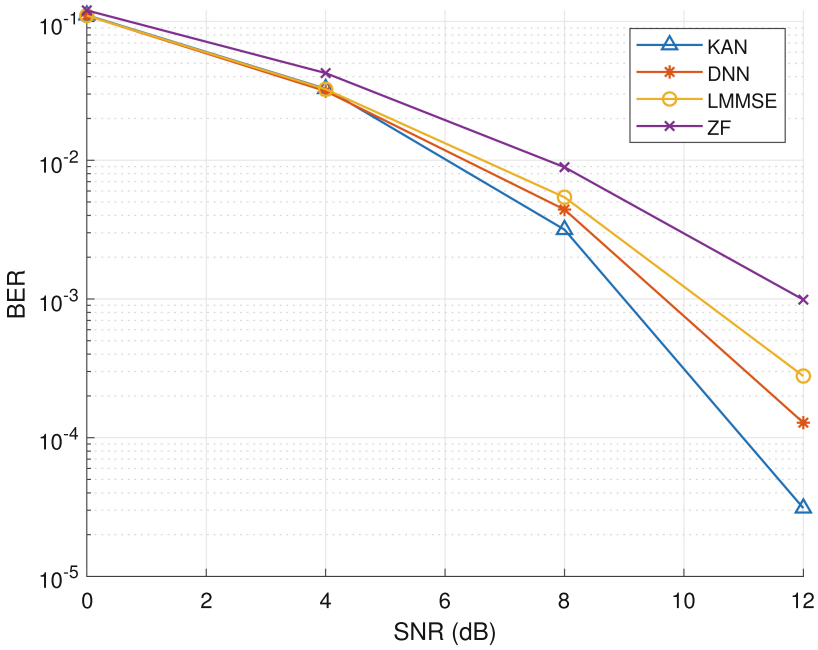

Fig. 6. 4-QAM BER comparison of the proposed KAN-based OTFS detector with LMMSE, ZF, DNN in LEO-Sat system, $M = 16, N = 8, CP = 5$.

accuracy. In contrast, due to their weaker nonlinear representation capabilities, the traditional LMMSE and ZF algorithms experience losses of 1 dB and 3 dB, respectively, compared to the KAN detector at the BER of 1×10^{-3}.

Additionally, the parameter count indicates a notable difference in the complexity of the algorithms, KAN has significantly fewer parameters than DNN, with about 328 k parameters compared with about 524 k parameters for DNN, KAN achieves more accurate results with fewer parameters, the KAN is significantly more parameter-efficient. Flexible and learnable activation functions allow KAN to achieve similar or higher prediction accuracy than DNN with fewer parameters. This makes KAN more suitable for deployment in satellite scenarios with limited computing and storage resources.

5 Conclusion

In this paper, an OTFS signal detection method for LEO-Sat system based on KAN network is proposed. Deploying the KAN completed with offline training online to the LEO-Sat communication system, the distorted signal at the receiver side can be effectively recovered and the system performance can be improved. Numerical results show that KAN has better BER performance than DNN, LMMSE and ZF. KAN achieve higher prediction accuracy with fewer parameters

than DNN. The proposed method effectively solves the problems existing in other traditional OTFS system signal detection methods, such as low detection accuracy and slow convergence speed. In this paper, the feasibility of KANs in LEO satellite communication signal detection research is proved, which offers a novel approach for future research in OTFS-based signal detection for LEO-Sat systems.

References

1. You, L., Li, K.X., Wang, J., Gao, X., Xia, X.G., Ottersten, B.: Massive MIMO transmission for LEO satellite communications. IEEE J. Sel. Areas Commun. **38**(8), 1851–1865 (2020)
2. Su, Y., Liu, Y., Zhou, Y., Yuan, J., Cao, H., Shi, J.: Broadband LEO satellite communications: architectures and key technologies. IEEE Wirel. Commun. **26**(2), 55–61 (2019)
3. Hadani, R., Monk, A.: OTFS: a new generation of modulation addressing the challenges of 5G. arXiv preprint arXiv:1802.02623 (2018)
4. Hadani, R., et al.: Orthogonal time frequency space modulation. In: 2017 IEEE Wireless Communications and Networking Conference (WCNC), pp. 1–6. IEEE (2017)
5. Devarajalu, S.K., Jose, D.: Performance evaluation of OTFS under different channel conditions for LEO satellite downlink. In: 2023 10th International Conference on Wireless Networks and Mobile Communications (WINCOM), pp. 1–6. IEEE (2023)
6. Gunturu, A., Godala, A.R., Sahoo, A.K., Chavva, A.K.R.: Performance analysis of OTFS waveform for 5G NR MMWAVE communication system. In: 2021 IEEE Wireless Communications and Networking Conference (WCNC), pp. 1–6. IEEE (2021)
7. Liu, Y., Chen, M., Pan, C., Gong, T., Yuan, J., Wang, J.: OTFS vs OFDM: which is superior in multiuser leo satellite communications. arXiv preprint arXiv:2403.02012 (2024)
8. Shi, J., et al.: OTFS enabled LEO satellite communications: a promising solution to severe doppler effects. IEEE Netw. (2023)
9. Raviteja, P., Phan, K.T., Jin, Q., Hong, Y., Viterbo, E.: Low-complexity iterative detection for orthogonal time frequency space modulation. In: 2018 IEEE Wireless Communications and Networking Conference (WCNC), pp. 1–6 (2018). https://doi.org/10.1109/WCNC.2018.8377159
10. Raviteja, P., Viterbo, E., Hong, Y.: OTFS performance on static multipath channels. IEEE Wirel. Commun. Lett. **8**(3), 745–748 (2019)
11. Murali, K.R., Chockalingam, A.: On OTFS modulation for high-doppler fading channels. In: 2018 Information Theory and Applications Workshop (ITA), pp. 1–10. IEEE (2018)
12. Raviteja, P., Phan, K.T., Hong, Y., Viterbo, E.: Interference cancellation and iterative detection for orthogonal time frequency space modulation. IEEE Trans. Wireless Commun. **17**(10), 6501–6515 (2018)
13. Zhang, X., Zhang, S., Xiao, L., Li, S., Jiang, T.: Graph neural network assisted efficient signal detection for OTFS systems. IEEE Commun. Lett. (2023)
14. Naikoti, A., Chockalingam, A.: Low-complexity delay-doppler symbol DNN for OTFS signal detection. In: 2021 IEEE 93rd Vehicular Technology Conference (VTC2021-Spring), pp. 1–6. IEEE (2021)

15. Enku, Y.K., et al.: Two-dimensional convolutional neural network-based signal detection for OTFS systems. IEEE Wirel. Commun. Lett. **10**(11), 2514–2518 (2021)
16. Tang, Y., Li, Y., Wang, X., Li, D.: Bi-lstm-based signal detection method for underwater acoustic OTFS communication system. In: 2023 International Conference on Microwave and Millimeter Wave Technology (ICMMT), pp. 1–3. IEEE (2023)
17. Liu, Z., et al.: KAN: Kolmogorov-Arnold networks. arXiv preprint arXiv:2404.19756 (2024)
18. Kolmogorov, A.N.: On the representation of continuous functions of several variables by superpositions of continuous functions of a smaller number of variables. American Mathematical Society (1961)
19. Braun, J., Griebel, M.: On a constructive proof of kolmogorov's superposition theorem. Constr. Approx. **30**, 653–675 (2009)
20. Vaca-Rubio, C.J., Blanco, L., Pereira, R., Caus, M.: Kolmogorov-Arnold networks (KANS) for time series analysis. arXiv preprint arXiv:2405.08790 (2024)
21. 3GPP TR 38.811 V15.4.0. Study on new radio (NR) to support non-terrestrial networks
22. Bora, A.S., Phan, K.T., Hong, Y.: Spatially correlated MIMO-OTFS for LEO satellite communication systems. In: 2022 IEEE International Conference on Communications Workshops (ICC Workshops), pp. 723–728. IEEE (2022)